



8. An Efficient Distributed Monitoring Framework for Reinforced Concrete Beam

Suresh Kumar KS.

*Lecturer, Department of Civil Engineering,
N. S. S. Polytechnic College, Pandalam,
Perumpulickal, Kerala, India.*

ABSTRACT

To strengthen the Reinforced Concrete (RC) structures, load carrying rate has to be determined with different tests. However, the manual test required a long time to value the cracking effectiveness. Considering that a novel Coati-based RC Strength Monitoring (CbRSM) framework was designed to estimate the RC beam strength. Moreover, Carbon Fibre Reinforced Polymer (CFRP) is employed as an adhesive agent to bond the concrete moulds. The obtained RC beams are tested in dual tests that are static and dynamic. After conducting the tests, the optimal coati function was activated for optimizing the sensing parameter to reduce power leakage. In contrast, the developed model was executed in the MATLAB programming language. In addition, to justify the effectiveness of the designed model, the key parameter of Accuracy was measured and compared with other models. Hence, the designed model shows the highest Accuracy of 98.3%, higher than the compared model.

KEYWORDS:

Reinforced Concrete, Distributed Sensor, Data Processing, Dead Load, Wind Load, Seismic Load.

1. Introduction:

In recent years, Reinforced Concrete (RC) interest increased due to its excellent mechanical specification compared to traditional concrete [1]. Reinforced concrete is known as reinforced cement concrete and ferroconcrete [2]. It is a composite material in which the low tensile strength remunerates by the inclusion of reinforcement having high-level tensile strength [3]. The concrete without using reinforcement has relatively more compressive strength but is very weak in tension [4]. Subsequently, steel has high tensile toughness, so it can resist the huge lateral exertion from pulling it apart. Combining these composite materials, achieving high strength and high tension capacity [5]. It contains steel beams, plates or fibre material.

It allows a load-carrying capacity to be well-suitable for any building construction. The current scenario is most frequently used in building materials [6]. It is widely used in large-scale constructions such as dams, bridges, stadiums, and large buildings. The structure of the reinforced concrete strength emerged in the construction activity to attain the upgraded design property and strength requirements because the environmental condition overlapped [7]. The structures required sustainable loads to challenge the environmental aspects [8]. Thus, strengthening properties must be needed in reinforced concrete to achieve the adequate strength specifications and extend the lifeline [9].

The RC materials include applying the external phase of the metallic plate and tensioning, mesh wire, jacketing and many more layers [10]. At the same time, satisfying all the required parameters, achieves high stiffness strength and becomes lightweight in material [11]. It can be produced fast and can produce low waste. Also, the material is low in cost and strength [12]. So currently, it is occupying many more construction points. Due to its low strength and cost, it is very economically efficient [13].

Structural monitoring is needed in reinforced concrete to measure and analyze structural health regarding strength and reliability [14]. With the help of distributed sensors, the structure loads have been monitored. The monitoring has been performed to analyze the dynamic forces and convert them into electric signals [15]. The technique is widely used in engineering to analyze structural changes and improve service life [16]. It collects quantitative and reliable information on the actual conditions of the building material [17]. Also, it detects the appearance of the construction industry. The monitoring model analyses the damage in the structure, damage situated part, and severity range of the damaged part and estimates the structures' lifetime [18].

The different loads to be monitored in the RC structure include dead, wind, and seismic loads [19]. The load monitoring is concentrated in RC structures to analyze the effect of the strength and remedial analysis in the dimension of the building material [20]. In this paper, an optimum proposed method is needed to effectively monitor the different loads in the RC structure with high reliability. The key factors involved in the proposed methodology are as follows,

- The ASTM C215 standard RC beam was initially considered for this study.
- Consequently, the CFRP was processed for the adhesive of the concrete blend then the static and dynamic tests were performed.
- Moreover, a novel CbRSM was developed to estimate the RC beam's vibration while applying the load.
- The vibration accelerometer was utilized every time vibration was sensed, and data was forwarded to the processing unit.
- Finally, the performance has been measured, such as Accuracy, cracking distance and displacement.

The remaining part of the paper was organized: Section 2 defines literature review studies with their outcomes. The materials and mix proportions are explained in Section 3. Section 4 discusses the experimental result and analysis. Finally, conclude with the conclusion in Section 5.

2. Related Works:

Some recent literatures related to monitoring in RC structures as discussed below,

Zhang et al. [21] designed a Seismic load monitoring system in reinforced concrete wall structures. Using the shaking table, the progressive seismic changes have been analyzed. Here, a grating sensor was used to monitor the damage in the structures. It enhances the sensitivity towards the structural material.

Also, it efficiently predicts the cracks inside the structures. It achieves high Accuracy and embedding ability. If any external cracks are developed in the structures, the sensor takes too long to provide the alert.

Bado et al. [22] developed a monitoring crack detection model in RC structures using distributed sensors. The six different cracking processes in the structures have been effectively monitored with the help of the required parameters. It achieves the maximum bond stress and minimum slip stress accordingly. It provides the remuneration between the structures and embedded bars. It allowed the constant monitoring of the mechanical strains of the structures. The fibre ability of the model is sufficient to analyze the performance. Moreover, the monitoring function is inefficient for analyzing the structures' health conditions.

Barrias et al. [23] implemented a Distributed optical fibre sensing (DOFS) model for analyzing the adhesive performance in the RC structures by the distributed fibre sensors. It monitors the different segments of the adhesives. This method analyses the three strain gauges used for the performance analysis. The spatial resolution and the data acquisition are well performed in this model. Finally, it achieves the performance of the adhesive used in different viscosity. It is very helpful to allow the adhesive in wider opening cracks. But the measurement of the cracked region shows a less accurate value.

Tan et al. [24] designed a Crack detection model for measuring and visualizing the strains and cracks in Fiber RC by distributed fibre sensors. Here two beams are prepared to reinforce polymer fibres. The distributed sensor is applied in compatible and realistic construction with the help of the beams. Subsequently, the beams are tested to bend the parameter. This method detects and locates the strains and cracks. It can easily detect small cracks before it is visualized. Moreover, it is very promising to reduce cost-related problems such as damage and loss than skilled workers. But more errors occurred in the calculation of the crack depth.

Siwowski et al. [25] designed the composite bridge monitoring model. Here, the monitoring model has been validated through the proof load. The suggested method is based on the Rayleigh scattering technique.

Here, consider two proof loads to evaluate the performance. Also, the two convolutional strain techniques are used to validate the system parameters. Thus, the Accuracy and spatial resolutions are greatly improved in this model. But the considered distribution monitoring is less efficient in this model for the construction sector.

3. Proposed CbDRM for Monitoring the Structure:

Ensuring a long lifetime of the building was expected to increase the service life and low maintenance cost. The RC structural monitoring collected continuous real-time data, and measuring the damage propagation using a proposed method was essential. Thus, a novel CbRSM framework was designed to monitor the structure accurately. The proposed methodology architecture is shown in Fig. 1.

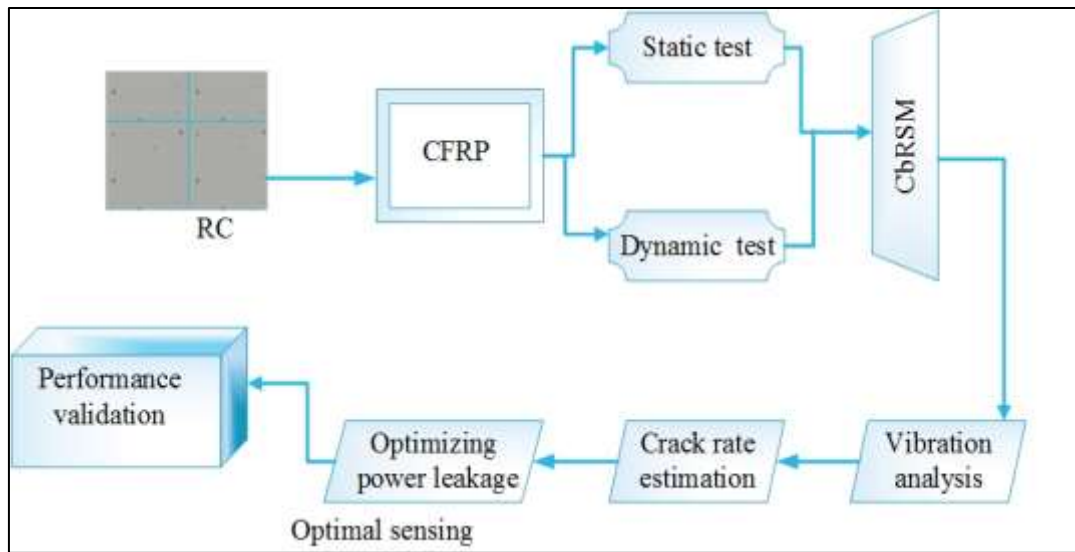


Figure 1: Proposed CbRSM Model

The multiple RC beam specimens are initially considered for this study with the accelerometer settings. Then carbon fibre is used as an adhesive agent to bond the concrete mould. Then to analyze the strength of the RC beam, load carrying strength test was performed according to the ASTM D3039 standard. Finally, the crack effectiveness was measured based on the crack displacement level. Finally, the monitoring effectiveness of the designed model is analyzed and compared through the accuracy parameter.

3.1 Materials:

The specimens of the reinforcement concrete beam were considered for this research program. From the ASTM C215 standard, the concrete beams were taken. In addition, the beam's minimum and maximum compressive strength are 15 MPa and 70 MPa, respectively. Moreover, the flexural strength of the concrete specimen is evaluated through the static and dynamic test, as per the ASTM C215 standard. The concrete strength test was carried out for 17 GPa to 34GPa. Also, the dimension size of the concrete reinforcement bar is 12mm and 15mm diameters.

For the crack monitoring and controlling process, the concrete is strengthened while the loads cross half portion from the predicted failure load. Here, the carbon FRP sheet was employed to strengthen the concrete beam and increase the flexural strength. Henceforth, the mechanical constraints of the CFRP are determined through the ASTM D3039 standard.

Table 1: RC bar specification

| Properties of RC bars | | |
|-----------------------|--------------|------------------|
| Diameter (mm) | Yield stress | Elasticity (MPa) |
| 12 | 50 | 216500 |
| 15 | 49 | 218464 |

According to the producer's instructions, panels of CFRP adhered to the testing frames. The type of glue used to adhere the CFRP material to a piece be hand-blended epoxy. Before adding the bonding agent, each concrete imperfection was eliminated using a handheld grinder. Henceforth, the bonding agent is applied uniformly with a brush to the cement base. The CFRP material was subsequently hand-laid to attain an exterior free of wrinkles. Using an inflatable roller, the air gap was eliminated among the mortar and CFRP sheeting. A thin epoxy film was applied to the CFRP sheet to enhance adhesion. The suggested curing period for the epoxy was a minimum of a week.

The CFRP, C-sheet 240 was considered for this study. The layer thickness of the sheet is 0.117mm, Strain 1.2 to 1.5% and the maximum tensile strength 3800MPa. In addition, the recorded maximum elasticity is 240 GPa.

Hence, the beam specimen constraints are described in Table 2. Here, the tensile centroid is 175mm, and the steel reinforcement compression is 25mm. Moreover, the CFRP width is 150mm for all samples. The static load progression was considered to find the beam's damage level at various load conditions. The beam was unloaded for each load balancing trial, and the dynamic test was performed.

Table 2: RC Beam specimen details

| Mixes | Specimen descriptions | | | | | | |
|-------|-----------------------|------------------------|-------------------------|--------------|-----------------------------------|-------------------------|---------------------------------|
| | Specimen | Load carrying capacity | Cubic compressive (MPa) | Air gap (mm) | Steel reinforcement cross-section | Centroid tensile stress | Steel reinforcement compression |
| D-1 | B1-15d | 0 | 20 | 100 | 225 | 175 | 225 |
| D-2 | B2-12d | 0 | 20 | 100 | 225 | 175 | 225 |
| D-3 | B3-15d | 1 | 47 | 200 | 400 | 175 | 400 |
| D-4 | B4-12d | 1 | 47 | 200 | 400 | 175 | 400 |

3.1.1 Static Test:

Utilizing a Linear Variable Differential Transformer (LVDT), motion transducers, and overload cells, respectively, the middle-span detours and loads placed in the cases were determined. A computer-assisted data collection system was used to record the resultant data. By the static test evaluation, it was measured that the beams are damaged continuously.

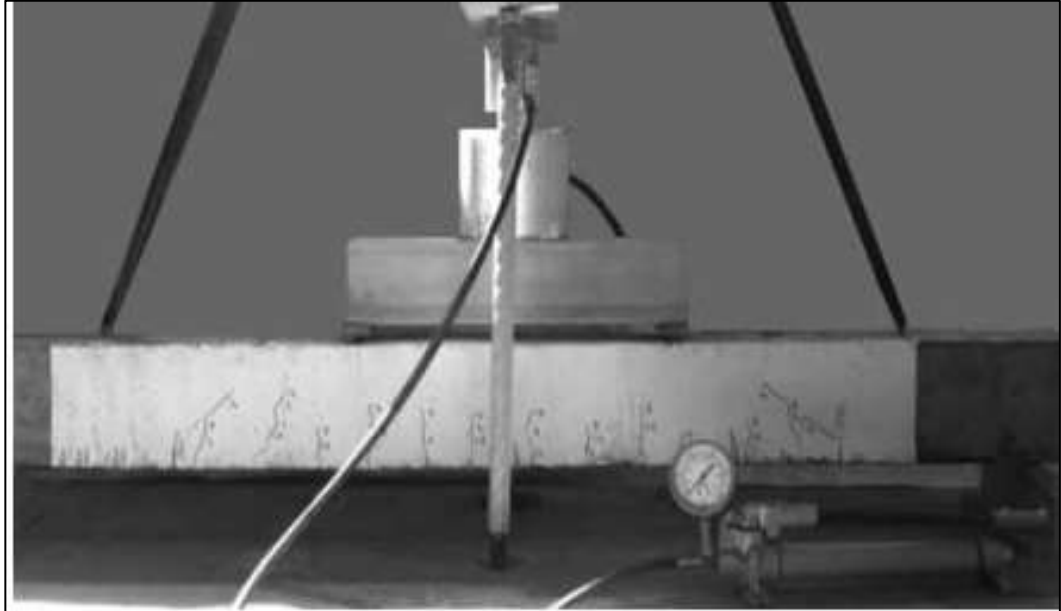


Figure 2: Equipment for Static Test

For the static test, the RC beam was tested statistically based on only beam weight at the initial loading stage L0 then the load was increased based on 10, 15, 20, 25,30..75. Here, the maximum applied load is 75 and the 11th, iteration that is L11 for the B4-12d specimen.

3.1.2 Dynamic Test:

A single acceleration sensor was used for recording the beams' movement. Every beam was regarded as a one-dimensional component, and its accelerometer was set along the horizontal axis of the topmost layer at the seventh level of motion.

The resulting stimulation forces were imparted to the shaft line via a 100 mm distance between each degree of motion. An electronic low-pass filter has been used on either input or output indications.

Through averaging frequency of 4095 Hz, 0–1550 Hz samples were gathered. An attack tip via the specified properties was created by analyzing various hammer points and taking into account the inherent harmonics of the supports. In addition, the hammer properties are 0 to 2kHz frequency range, 0.57ms pulse duration and 300 to 100N force range. Also, the metallic specification of the hammer is plastic.

3.2 CbRSM Optimal Vibration Analysis:

During a ten-day span, the beam's vibrational characteristics were determined. After 10 days, the unoccupied beam's eigenvalue was observed to have altered considerably. Frequencies from nature are affected by concrete getting older and bearings; in execution, these variables have a more complex effect on the reactivity of building materials.

Notably, the experiments were conducted throughout summertime via a substantial temperature difference at each point of tests, yet no numerical information on the temperature difference was collected. Sensing the concrete crack points and transferring them to the measurement points require more power spectrum that leads to cause power leakage of the accelerometer.

Hence, to optimize the accelerometer performance, coati optimal function was considered. To predict the cracking effect and the distance, the vibration data should be accurate at a low cost. Hence, the vibration rate estimations are defined by eqn. (1).

$$V_A = load + a_g (C_s - C_r) \quad (1)$$

Here, the vibration analysis variable is exposed as V_A , cracking rate is defined as C_r , C_s is the compressive strength and the air gap is exposed as a_g . Moreover, the cracking rate was determined by eqn. (2).

$$C_r = C_d + load(C_s - S_f) \quad (2)$$

Here, the concrete displacement is exposed as C_d and the flexural strength is determined as S_f . Hence, by processing eqn. (2) the cracking rate was established. Henceforth, the cracking distance is described by eqn. (3).

$$C_d = load + C_s(C_l - O_l) \quad (3)$$

Here, the cracked concrete length is exposed as C_l and the original concrete length is O_l . Crack displacement was measured by taking the difference between the original and cracked concrete length with respect to load and compressive strength. In addition, the vibration sensing accelerometer needed more p

ower to complete the vibration analysis task. The high power consumption of the sensing element caused high power leakage. Considering that, the principle of coati algorithm has processed optimal sensing. Here, O_s denotes the optimal sensing and P represents power utilization. Hence, optimal sensing is carried out by eqn. (4).

$$O_s = \begin{cases} P(V_A) \leq 2 & \text{optimal} \\ else & \text{max imum} \end{cases} \quad (4)$$

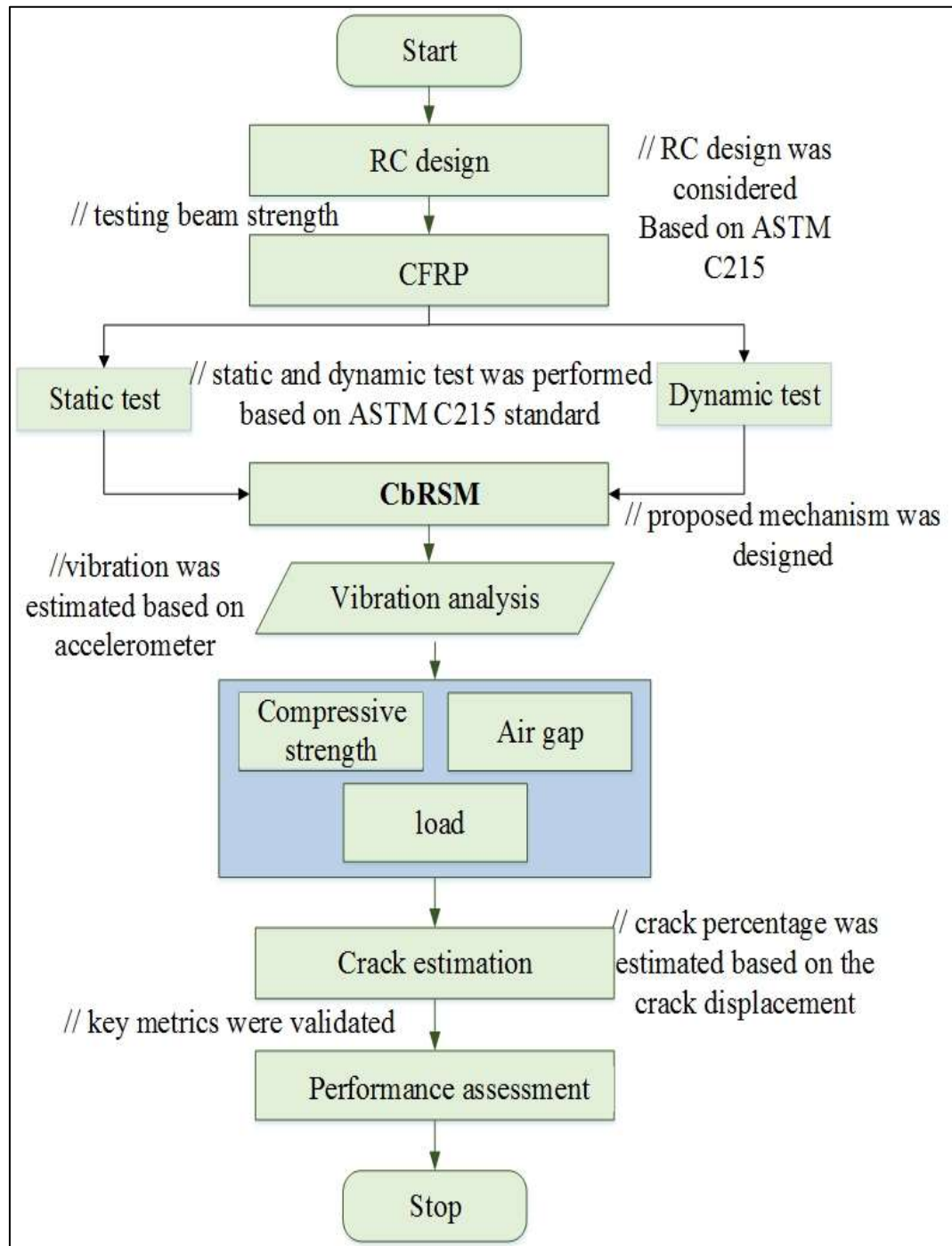


Figure 3: Flowchart of CbRSM

The steps and processes presented in the designed model were detailed in algorithm 1 and Fig. 3. Based on these step processes, the MATLAB code was executed, and the results were verified. The algorithm incorporated all mathematical function parameters in the pseudocode format.

Algorithm. 1 CbRSM

Start

{

Design of RC with accelerometer

Vibration analysis ()

{

int $V_A, a_g, C_s, C_r;$

// vibration analysis variables were initialized using coati initialization process

$V_A \rightarrow load + damage$

// based on the applied load and first damage occurrence, the vibration percentage was recorded.

}

Crack rate and distance estimation ()

{

$C_r \rightarrow diff(C_s \ \& \ S_f)$

// here, the cracking rate was estimated by eqn. (2)

$C_d \rightarrow distance(C_l)$

//cracking distance was analyzed using eqn. (3)

}

Optimal sensing ()

{

int $O_s, P;$

// initializing the optimal sensing parameter

if ($P(V_A) \leq 2$)

{

Optimal

}else(maximum)

}

Stop

4. Result and Discussion:

The developed technique was implemented in the MATLAB platform. This implementation process was running on the Windows 10 platform. The process of this work was to perform the RC structural monitoring. Vibration-based detection methods are useful for finding structural property changes resulting from damage and reinforcement. The variances in stiffness induced by breaking and reinforcing can be measured using identification techniques based on vibrations or pattern structures. In this investigation, both static and dynamic experiments were carried out upon beams enhanced with CFRP panels.

4.1 Case Study:

The amplitudes are impacted by destruction and enhancement, but the exact places of damage do not affect their alterations. The incidences decrease as damage increases, but the surroundings additionally influence them. It is generally accepted that the outside temperature and other external factors influence the dynamic properties of most engineering structures. Therefore, vibrations from nature are ineffective for identifying damage in unregulated environments. To analyze the working procedure of the proposed design, different tests were made with different loads and the outcomes were mentioned as follows,

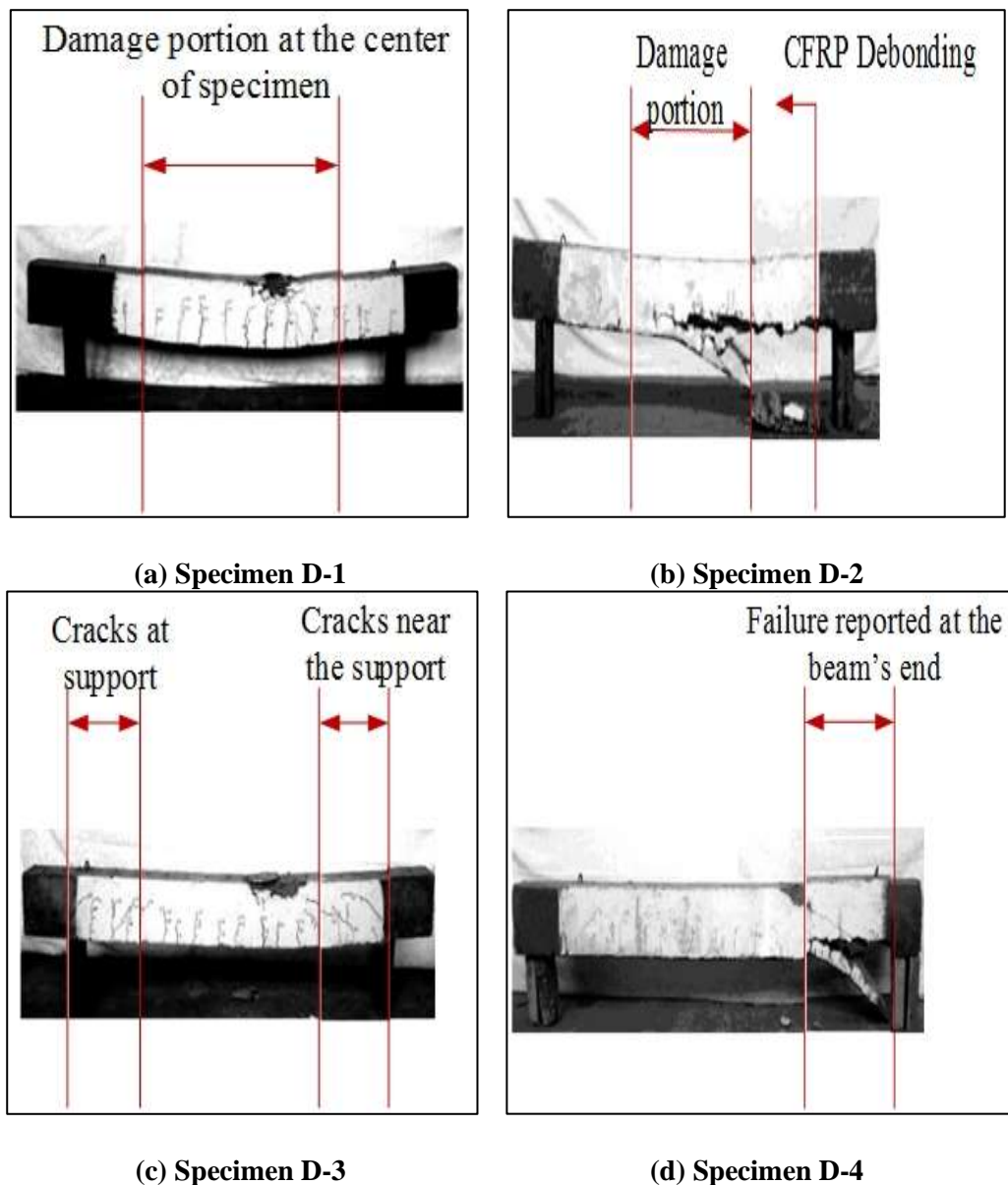


Figure 4: Beams after failure

The damaged area of specimen B1-15d was in the unsymmetrical and middle span. Significant diagonal cracking was observed to occur around the right-hand side of B2-12d specimen. Furthermore, specimen B3-15d attains the crack near the support on the right and left sides of the specimen. Also, specimen B4-15d failed from its right end. Moreover, the representation of beams after failure is illustrated in Fig. 4.

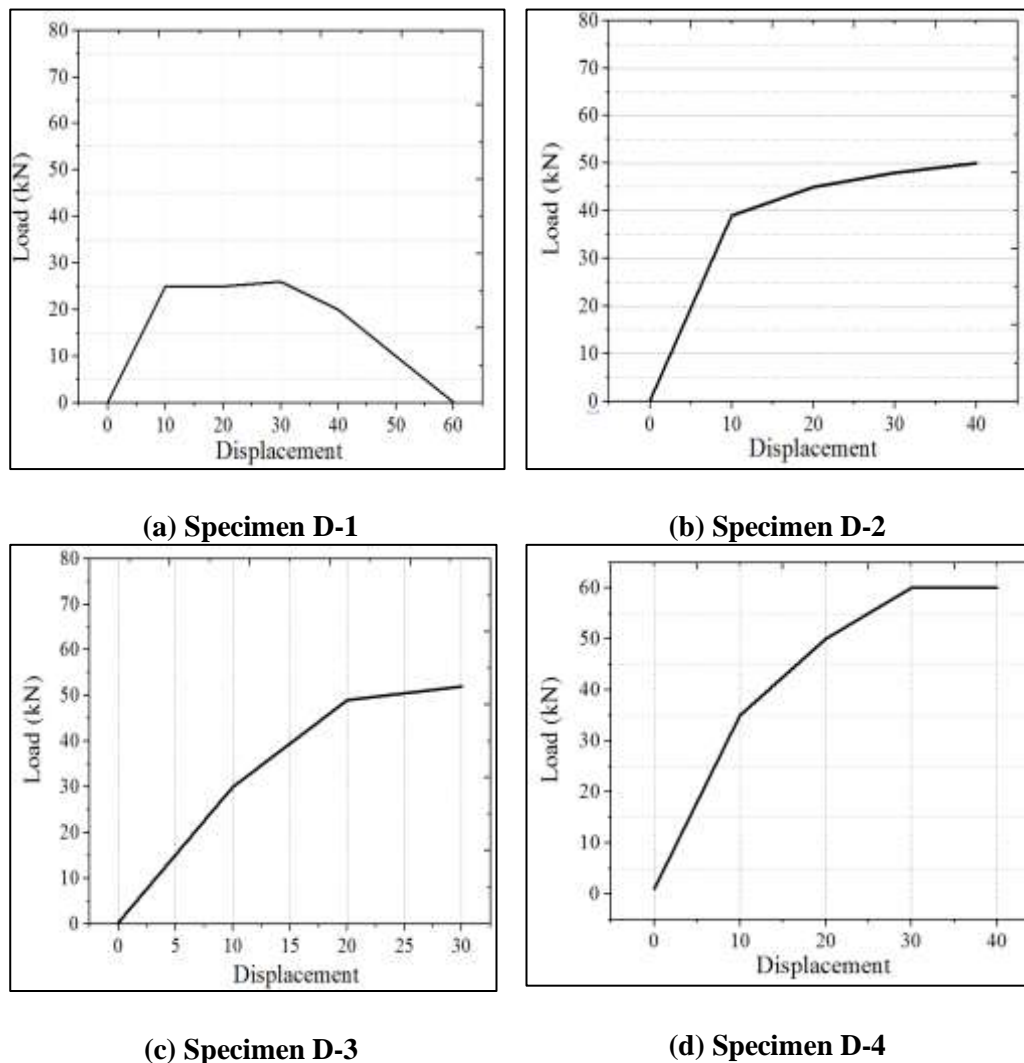


Figure 5: The relationship of load displacement for beam specimens

During static loading, the beams were subsequently smashed. Here, apply two load steps, beam weight and similar load, before strengthening the specimens. Furthermore, the relationship between the load and displacement of the specimens such as specimens B1-15d, B2-12d, B3-15d, and B4-15d was shown in Fig. 5. The dependability of oscillatory identification of parameters in the unscathed state was confirmed through both theoretical and scientific investigations. The practical on dynamic test outcomes contrasted with the academic vibrating beam versions depending on the Timoshenko and Euler–Bernoulli beam ideas and analyzed.

The contrasts demonstrated that modal parameter detection is reasonably precise. The findings of the finite-element framework of oscillating beam samples were consistent regarding the experimental outcomes.

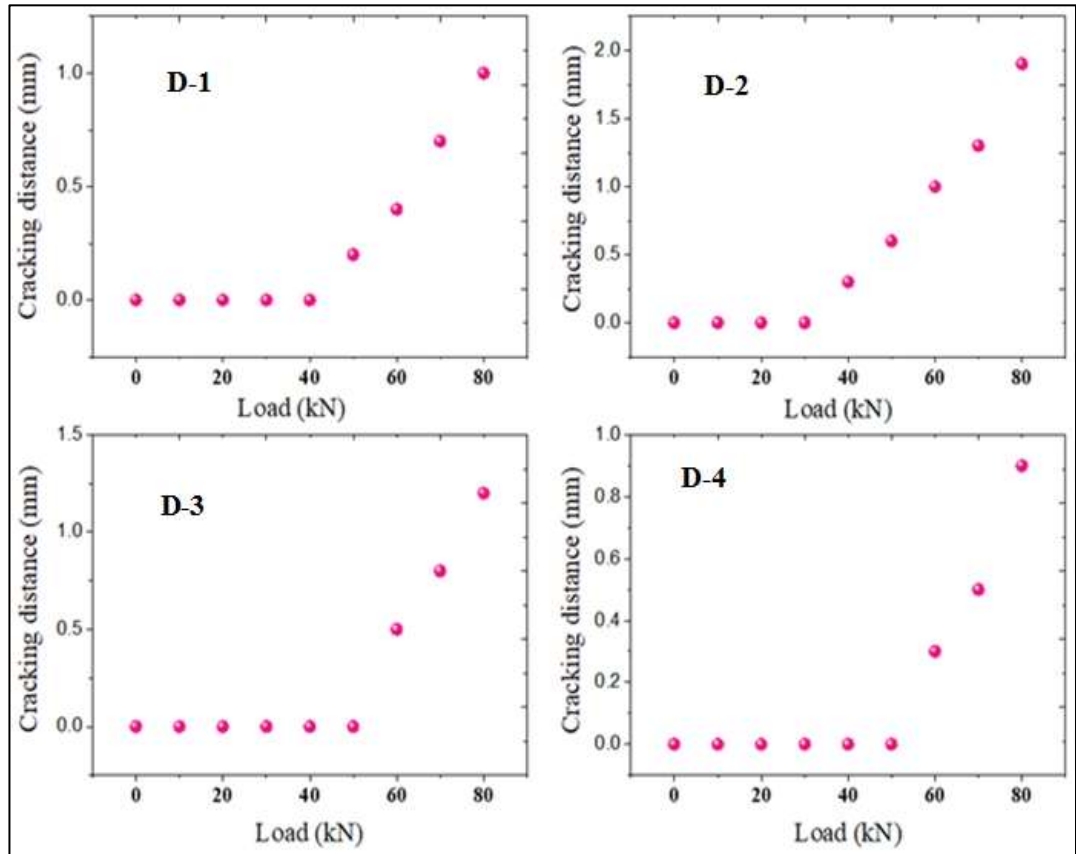


Figure 6: cracking rate estimation

The crack distance was measured for every four mixes; in the B4-15d specimen reported less crack distance score than the other specimens. That validation outcome is exposed in Fig. 6 and Table 3. The dynamic elasticity describes an almost entirely elastic result and is unaffected by creep, contraction, or additional phenomena. A minor decrease in modulus of motion caused by creep, compression, or other occurrences may be accounted for in the current study because building materials stresses throughout initial-state shaking experiments are tiny. Regarding concrete variability and endurance, the dynamic modulus of aggregate in 55 MPa and 18 MPa capacities was decreased by 5 to 10%.

In the proposed CbDRM technique, the accurate performance outcome of optimizing the RC structure was provided with various metrics, including precision, recall, Accuracy and F-score. Then, the system was compared with several existing techniques such as Deep Convolution Neural Network (DCNN) [26], Incremental random Sampling (IRS) [27], Shallow Convolution Neural Network (SCNN) [28], Semantic Segmentation Network (SegNet) [29].

Table 3: Cracking distance estimation

| Cracking distance | | | | |
|-------------------|-----|-----|-----|-----|
| Load (kN) | D-1 | D-2 | D-3 | D-4 |
| 0 | 0 | 0 | 0 | 0 |
| 10 | 0 | 0 | 0 | 0 |
| 20 | 0 | 0 | 0 | 0 |
| 30 | 0 | 0 | 0 | 0 |
| 40 | 0 | 0.3 | 0 | 0 |
| 50 | 0.2 | 0.6 | 0 | 0 |
| 60 | 0.4 | 1 | 0.5 | 0.3 |
| 70 | 0.7 | 1.3 | 0.8 | 0.5 |
| 80 | 1 | 1.9 | 1.2 | 0.9 |

The presented model recorded the highest vibration analysis accuracy at 98.3%, which is quite higher than the compared models. Hence, the obtained coati optimization performed better than the other intelligent and sampling methods.

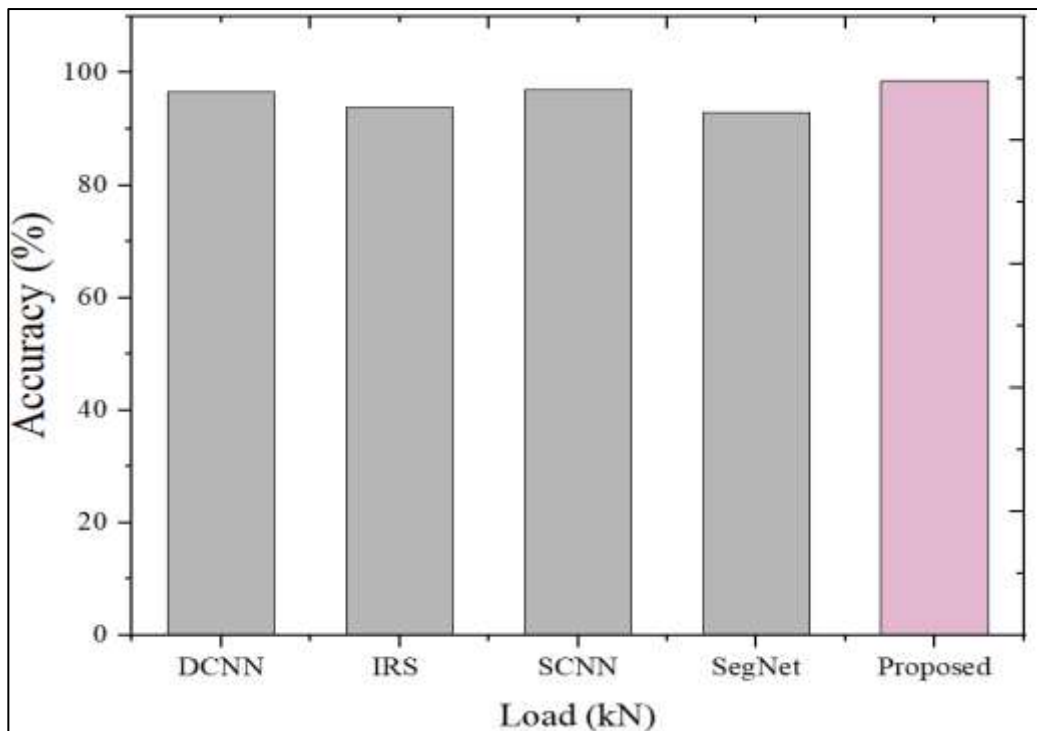


Figure 7: Accuracy comparison

5. Conclusion:

This paper describes the RC strength analysis study based on the ASTM standard with the CFRP sheet. Moreover, the static and dynamic test was carried out, and the results were described. Finally, the power leakage was optimized by optimal sensing formulation from the coati algorithm. In addition, the cracking distance is measured considering load in kN. The highest cracking distance was reported for the D-2 mix specimen; the recorded highest distance is 1.9mm. Moreover, the Accuracy is measured for the novel CbRSM for the monitoring function. The proposed framework has scored the finest exactness rate at 98.3%. The vibration analysis accuracy was improved by 1% compared to the previous studies. However, optimizing the cracking rate is not established in this RC study. In future, implementing the optimal selection and fine replacement procedure in the RC beam will improve the load handling capacity by maximizing the compressive strength and flexural rate.

Reference:

1. Chou, J.S., Karundeng, M.A., Truong, D.N., Cheng, M.Y.: Identifying deflections of reinforced concrete beams under seismic loads by bio-inspired optimization of deep residual learning. *Struct. Control Health Monit.* 29(4), e2918 (2022).
2. Zhou, K., Lei, D., He, J., Zhang, P., Bai, P., Zhu, F.: Real-time localization of micro-damage in concrete beams using DIC technology and wavelet packet analysis. *Cem. Concr. Compos.* 123, 104198 (2021).
3. Das, A., Maity, D., Bhattacharyya, S.K.: Investigation on the efficiency of deep liquid tanks in controlling dynamic response of high-rise buildings: A computational framework. *Structures*, Elsevier, Vol. 37, pp. 1129-1141 (2022).
4. Mankar, A., Bayane, I., Sørensen, J.D., Brühwiler, E.: Probabilistic reliability framework for assessment of concrete fatigue of existing RC bridge deck slabs using data from monitoring. *Eng. Struct.* 201, 109788 (2019).
5. Reboul, N., Grazide, C., Roy, N., Ferrier, E.: Acoustic emission monitoring of reinforced concrete wall-slab connections. *Constr. Build. Mater.* 259, 119661 (2020).
6. Mishra, M., Lourenço, P.B., Ramana, G.V.: Structural health monitoring of civil engineering structures by using the internet of things: A review. *J. Build. Eng.* 48, 103954 (2022).
7. Chen, L., Chen, W., Wang, L., Zhai, C., Hu, X., Sun, L., Tian, Y., Huang, X., Jiang, L.: Convolutional neural networks (CNNs)-based multi-category damage detection and recognition of high-speed rail (HSR) reinforced concrete (RC) bridges using test images. *Eng. Struct.* 276, 115306 (2023).
8. Zdanowicz, K., Gebauer, D., Koschemann, M., Speck, K., Steinbock, O., Beckmann, B., Marx, S.: Distributed fiber optic sensors for measuring strains of concrete, steel, and textile reinforcement: Possible fields of application. *Struct. Concr.* (2022).
9. Siahkouhi, M., Razaqpur, G., Hout, N.A., Baghban, M.H., Jing, G.: Utilization of carbon nanotubes (CNTs) in concrete for structural health monitoring (SHM) purposes: A review. *Constr. Build. Mater.* 309, 125137 (2021).
10. Heitner, B., O'Brien, E.J., Yalams, T., Schoefs, F., Leahy, C., Décatore, R.: Updating probabilities of bridge reinforcement corrosion using health monitoring data. *Eng. Struct.* 190, 41-51 (2019).

11. Lu, X., Guan, H., Sun, H., Li, Y., Zheng, Z., Fei, Y., Yang, Z., Zuo, L.: A preliminary analysis and discussion of the condominium building collapse in surfside, Florida, US, June 24, 2021. *Front. Struct. Civ. Eng.* 15, 1097-110 (2021).
12. Al-Rousan, R.Z.: Cyclic behavior of alkali-silica reaction-damaged reinforced concrete beam-column joints strengthened with FRP composites. *Case Stud. Constr. Mater.* 16, e00869 (2022).
13. Ma, G., Du, Q.: Structural health evaluation of the prestressed concrete using advanced acoustic emission (AE) parameters. *Constr. Build. Mater.* 250, 118860 (2020).
14. Thirumalaiselvi, A., Sasmal, S.: Pattern recognition enabled acoustic emission signatures for crack characterization during damage progression in large concrete structures. *Appl. Acoust.* 175, 107797 (2021).
15. De Maio, U., Greco, F., Leonetti, L., Blasi, P.N., Pranno, A.: A cohesive fracture model for predicting crack spacing and crack width in reinforced concrete structures. *Eng. Fail. Anal.* 139, 106452 (2022).
16. Saliba, J., Mezhoud, D.: Monitoring of steel-concrete bond with the acoustic emission technique. *Theor. Appl. Fract. Mech.* 100, 416-25 (2019).
17. Mansourdehghan, S., Dolatshahi, K.M., Asjodi, A.H.: Data-driven damage assessment of reinforced concrete shear walls using visual features of damage. *J. Build. Eng.* 53, 104509 (2022).
18. Wojtczak, E., Rucka, M., Skarżyński, Ł.: Monitoring the fracture process of concrete during splitting using integrated ultrasonic coda wave interferometry, digital image correlation and X-ray micro-computed tomography. *NDT & E Int.* 126, 102591 (2022).
19. Ai, D., Cheng, J.: A deep learning approach for electromechanical impedance based concrete structural damage quantification using two-dimensional convolutional neural network. *Mech. Syst. Signal Process.* 183, 109634 (2023).
20. Tan, X., Guo, P., Zou, X., Bao, Y.: Buckling detection and shape reconstruction using strain distributions measured from a distributed fiber optic sensor. *Measurement* 200, 111625 (2022).
21. Zhang, C., Alam, Z., Sun, L., Su, Z., Samali, B.: Fibre Bragg grating sensor-based damage response monitoring of an asymmetric reinforced concrete shear wall structure subjected to progressive seismic loads. *Struct. Control Health Monit.* 26(3), e2307 (2019).
22. Bado, M.F., Casas, J.R., Kaklauskas, G.: Distributed Sensing (DOFS) in Reinforced Concrete members for reinforcement strain monitoring, crack detection and bond-slip calculation. *Eng. Struct.* 226, 111385 (2021).
23. Barrias, A., Casas, J.R., Villalba, S.: Distributed optical fibre sensors in concrete structures: Performance of bonding adhesives and influence of spatial resolution. *Struct. Control Health Monit.* 26(3), e2310 (2019).
24. Tan, X., Abu-Obeidah, A., Bao, Y., Nassif, H., Nasreddine, W.: Measurement and visualization of strains and cracks in CFRP post-tensioned fiber reinforced concrete beams using distributed fiber optic sensors. *Autom. Constr.* 124, 103604 (2021).
25. Siwowski, T., Rajchel, M., Howiacki, T., Sienko, R., Bednarski, Ł.: Distributed fibre optic sensors in FRP composite bridge monitoring: Validation through proof load tests. *Eng. Struct.* 246, 113057 (2021).
26. Ali, L., Alnajjar, F., Jassmi, H.A., Gocho, M., Khan, W., Serhani, M.A.: Performance evaluation of deep CNN-based crack detection and localization techniques for concrete structures. *Sensors* 21(5), 1688 (2021).

27. Zhang, J., Yang, X., Li, W., Zhang, S., Jia, Y.: Automatic detection of moisture damages in asphalt pavements from GPR data with deep CNN and IRS method. *Autom. Constr.* 113, 103119 (2020).
28. Kim, B., Yuvaraj, N., Sri Preethaa, K.R., Arun Pandian, R.: Surface crack detection using deep learning with shallow CNN architecture for enhanced computation. *Neural. Comput. Appl.* 33, 9289-305 (2021).
29. Chen, T., Cai, Z., Zhao, X., Chen, C., Liang, X., Zou, T., Wang, P.: Pavement crack detection and recognition using the architecture of segNet. *J. Ind. Inf. Integr.* 18, 100144 (2020).